Experimental Assessment of the Performance of an Electron Cyclotron Resonance Acceleration (ECRA) Thruster Operated with Iodine

Experimental Assessment of the Performance of an Electron Cyclotron Resonance Acceleration (ECRA) Thruster Operated with Iodine

Samuele Carere*†, Federico Boni*, Guido Lombardi †, Victor Désangles*
* Physics Instrumentation and Space Department, ONERA, Université Paris-Saclay, 91123 Palaiseau, France
† Dipartimento di Elettronica, Politecnico di Torino, 10129 Torino, Italy
contact author: victor.desangles@onera.fr

***Abstract*—The growing demand for compact and efficient space propulsion systems has accelerated the development of alternative propellants and thruster technologies. Iodine is a promising candidate for electric propulsion due to its high storage density, low ionization energy, and significantly lower cost compared to xenon. This work explores the use of iodine in an Electron Cyclotron Resonance Acceleration (ECRA) thruster originally designed for xenon. Thrust, specific impulse, and efficiency were measured using a Faraday probe for iodine and other propellants. The results, however subject to large uncertainties due to the estimation method of ion energy, demonstrate the similar behavior of ECRA thruster between iodine and xenon. Performance uncertainties related to plasma composition are discussed.**

***Index Terms*—electric propulsion, iodine plasma, electrodeless thruster, magnetic nozzle, thrust efficiency**

I. Introduction

OVER the past few decades, the rapid growth of the new space economy has increased the demand for cost efficient propulsion systems. In this context, electric propulsion (EP) has emerged as a viable alternative to traditional chemical propulsion, both for orbit-raising and station-keeping maneuvers and for all kind of satellite mission, from geostationary to very low earth orbit. Although EP systems generate lower thrust, they offer key advantages such as higher specific impulse and improved mass utilization efficiency, resulting in a considerable reduction in the required propellant mass for a given mission. Electric propulsion systems operate by using electrical energy produced on board to create and accelerate a plasma to generate thrust. Within the current technological landscape, iodine is attracting growing interest as a propellant. Its high storage density, solid-state storage capability, low cost, and abundant availability on Earth make it a promising alternative to xenon, the conventional propellant used in EP systems.

This project investigates the use of iodine in electric propulsion, focusing on the first tests of the Electron Cyclotron Resonance Acceleration (ECRA) thruster originally developed for xenon and operated with iodine. This work aims at estimating if iodine is an interesting substitute to xenon to operate an electrodeless plasma thruster such as the ECRT.

II. Comparison of iodine and xenon properties relevant for Electric Propulsion

A comparison between xenon and iodine as propellants highlights the growing interest in iodine for electric propulsion applications. While xenon is chemically inert, gaseous under standard conditions, and supported by a solid experimental background, it suffers from limited availability, high cost (around 3600 €/kg), and the need for high-pressure storage systems.

In contrast, iodine offers several advantages: it is widely available on Earth, significantly more affordable (around 480 €/kg), and can be stored in solid form at ambient pressure, simplifying tank design in terms of volume and weight. Additionally, iodine has an atomic mass comparable to xenon and a lower ionization energy, potentially enhancing thruster efficiency. However, iodine also presents specific challenges. It requires heating to transition to the gaseous phase, it is chemically reactive and corrosive, and lacks standardized experimental data and compatible materials. Furthermore, iodine naturally exists in a molecular form (I_2), and the complex chemical reactions occurring in the plasma must be thoroughly understood and controlled to enable precise development and optimization of EP engines.

A comparative overview of xenon and iodine properties relevant to electric propulsion is reported in Table I. Despite its limitations, iodine emerges as a compelling alternative to xenon, particularly for miniaturized and cost-effective spacecraft propulsion systems.

TABLE I
Comparison between xenon and iodine relevant properties for electric propulsion applications.

Property	Xenon (Xe)	Iodine (I)
Atomic mass [u]	131.3	126.9
First ionization energy [eV]	12.1	10.5 (9.4 for I_2)
Vapor pressure temp. at 10^{-6} Torr [K]	58.2	199.5
Physical state at standard conditions	Gas	Solid
Storage	Pressurized tanks	Unpressurized
Corrosiveness	Inert	Corrosive
Experimental data availability	High	Limited
Cost [€/kg]	3600	480
Availability on Earth	Low	High

III. Electric propulsion fundamental and thruster performance parameters

Electric propulsion devices produce thrust by accelerating and ejecting ionized propellant, converting a loss of mass into spacecraft acceleration. The thrust is defined as the rate of change of propellant momentum and can be expressed as:

$$T = \frac{d}{dt}(mv_{ex}) = \dot{m}v_{ex}, \tag{1}$$

where T is the thrust, $\dot{m}$ is the propellant mass flow rate, and v_{ex} is the propellant exhaust velocity relative to the spacecraft.

The relation between the spacecraft change of velocity and the propellant consumption is given by the rocket equation:

$$\Delta v = v_{\text{ex}} \ln\left(\frac{m_0}{m_f}\right), \tag{2}$$

where m_0 and m_f are the initial and final spacecraft masses, including propellant.

In this work, several parameters will be used to characterize the thruster performance. Firstly, a fundamental parameter is the specific impulse I_{sp}, which identifies the efficiency in the use of propellant mass to produce thrust:

$$I_{\text{sp}} = \frac{T}{g_0\dot{m}} = \frac{v_{\text{ex}}}{g_0}, \tag{3}$$

where g_0 is the standard gravitational acceleration.

Mass utilization efficiency indicates how much of the injected mass is effectively ionized to produce thrust. Under the assumption of a plasma consisting only of singly-charged ions, it reads:

$$\eta_m = \frac{\dot{m}_i}{\dot{m}} = \frac{I_b}{e}\frac{M}{\dot{m}}, \tag{4}$$

where I_b is the ion beam current, M is the ion mass, and e is the elementary charge.

The energy efficiency is the ratio of the output power ejected through the plume and the input power injected in the plasma:

$$\eta_e = \frac{P_b}{P_{elec}} = \frac{E_i \cdot I_b}{P_{elec}}, \tag{5}$$

where P_{elec} is the electrical power supplied to the thruster.

The divergence efficiency quantifies the ratio between the actual thrust and the ideal thrust that would be obtained if all the ions were ejected along the thrust axis.

$$\eta_d = \frac{T}{\dot{m}_i u_i} = \sqrt{\frac{e}{2M}} \cdot \frac{T}{\sqrt{E_i} I_b} \tag{6}$$

The total (or thrust) efficiency η_T combines the effects of the above mentioned efficiencies and indicates the fraction of input power converted into kinetic power directed on axis:

$$\eta_T = \frac{T^2}{2\dot{m}P_{\text{elec}}} = \eta_m\eta_e{\eta_d}^2. \tag{7}$$

Last, the thrust-to-power ratio (TTPR) quantifies how efficiently thrust is produced per unit of injected power:

$$\text{TTPR} = \frac{T}{P_{\text{elec}}} = \frac{2\eta_T}{g_0 I_{\text{sp}}}. \tag{8}$$

IV. State-of-the-art of iodine Electric Propulsion

Studies on iodine-fueled Hall Effect Thrusters (HETs) have demonstrated performance similar to xenon, with iodine often outperforming xenon at higher voltages. Hillier *et al.* [1] and Szabo *et al.* [2], [3] reported comparable thrust-to-power ratios (TTPR) and higher efficiencies at voltages above 300 V. Szabo's work also highlighted iodine's reduced ion beam divergence at high voltages and the effects of iodine exposure on thruster materials, showing significant oxidation of iron but stability of nickel coatings.

Gridded ion thrusters and radio-frequency (RF) ion thrusters have shown possible enhanced performance when operated with iodine compared to xenon. Grondein *et al.* [4] predicted higher efficiency at low mass flow rates for iodine compared to xenon. Holste *et al.* [5] and Yang *et al.* [6] confirmed these findings, noting that iodine achieves higher thrust than xenon at higher RF load powers but lower thrust at low powers, with comparable TTPRs around 24 mN/kW.

Iodine's higher storage density significantly reduces the volume required for spacecraft propellant, offering major advantages for mission design and cost efficiency. For example, asteroid retrieval missions may require substantially less iodine compared to xenon [3].

Recently, iodine propulsion achieved operational readiness with the successful in orbit demonstration of an NPT30-I2 iodine thruster of the company ThrustMe [7].

V. Experimental Apparatus

A. The vacuum facility

Experiments were conducted in the BEPI ONERA Facility: a cylindrical vacuum chamber with an internal diameter of 0.65 m and length of 1 m. The chamber achieves low-pressure conditions through a three-stage pumping system. The schematics of the facility is shown in Fig. 1. First, a primary pump reduces pressure from 1 atmosphere to the 10^{-1}–10^{-2} mbar range. Then, a turbomolecular pump further reduces the pressure to around 10^{-7} mbar. Finally, a cryogenic system is used to maintain a 0.6 m^2 panel at a constant temperature of $-70°$C (200 K) using ethanol coolant. At this temperature, the iodine vapor pressure is 10^{-6} mbar, enabling efficient iodine condensation and increasing the total pumping speed from about 1000 to about 5600 L/s. For low pressure operation with iodine propellant, the vacuum gauges appears to give unreliable data for currently unknown reasons. Gauges' surfaces poisoning is suspected and experiments are currently conducted heating the gauges tubing. For the other gases used, the cryogenic panel is not cold enough to be effective. As a results, the effective pumping speed is reduced, with values of 1050 L/s for xenon, 1080 L/s for argon, and 1690 L/s for nitrogen.

B. ECRA thruster

The Electron Cyclotron Resonance Acceleration (ECRA) thruster, depicted on the schematic on Figure 2, is an electrodeless thruster which has been developed at ONERA since 2010 [8]–[12]. It operates based on the resonant absorption of microwaves by electrons to generate plasma, and on the

acceleration of electrons and ions in a magnetic nozzle, therefore generating thrust. Neutral gas is injected into a coaxial structure, the plasma source, where about 30 W of microwave power at 2.45 GHz are deposited into the plasma. A permanent magnet is placed at the back of the thruster creates both the electron cyclotron resonance region inside the source and the diverging magnetic nozzle. In the resonance region (around 875 G), the electron cyclotron frequency matches the microwave frequency, enabling efficient electron heating and plasma generation. The thruster body is electrically floating, so that the plasma plume remains current-free. It has been demonstrated that the ECRA thruster performance is highly sensitive to the testing environment, particularly to background pressure and facility dimensions [13]. To date, the highest performance figures have been achieved in the large JUMBO facility at Justus Liebig University [12]. The performance data presented in this work fall below those benchmarks due to limitations in facility size and achievable vacuum pressure.

C. Iodine injection line

The iodine injection line is composed of a sublimation vial, a condensable mass flow meter MKS-1150C, and a set of heated tubing. The gas line is heated to ensure iodine remains in its gaseous phase from the vial to the thruster. The line is divided into four independently controlled zones. Each zone consists of a heating patch, a PT-1000 thermocouple with an accuracy of ±0.1°C, and a relay that regulates the heating patch to maintain the desired temperature. We find that the optimal configuration to minimize iodine condensation in the tubes is a positive temperature gradient, starting at 95°C at the iodine reservoir and gradually increasing to 101°C at the thruster.

D. Plasma and thruster diagnostics

In this work, the two measured quantities are the thruster floating potential and ion current density. Thruster floating potential is measured using a voltmeter. The ion current density is measured using a Faraday cup developed by Pioch *et al.* [14]. The probe is mounted on a rotating arm centered on the plasma source region of the thruster. The arm and the acquisition circuit of the probe are computer-controlled, allowing for angular scan data acquisition from $-90°$ to $+90°$ relative to the thruster symmetry axis, as illustrated in Fig. 1. The probe collector is biased at -300 V using a high-voltage

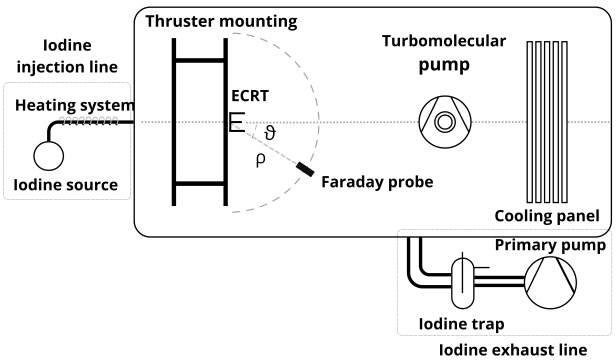

Fig. 1. Schematic view of the iodine vacuum chamber.

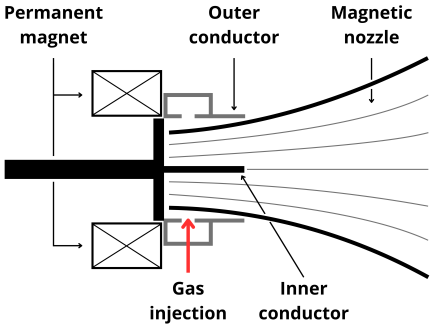

Fig. 2. Schematic of the ECR thruster.

Fig. 3. Photo of ECRA thruster operated with iodine inside ONERA facility, at a volume flowrate of 1.5 sccm, 25 W of input power, at a pressure of $1.65{\cdot}10^{-5}$ mbar (without cryogenic system).

power supply powered by electrically floating batteries to reduce electrical noise. The value of the collector bias ensures complete repulsion of high-energy electrons (tens of eV) while enabling accurate estimation of the local ion flux emitted by the thruster. The collected ion current is measured through a 680 kΩ shunt resistor. The background offset signal is removed from the collected ion current profiles, and the signal is then averaged by using a Savitzky–Golay filter (window length = 501 and polynomial degree = 3) to reduce noise and ensure reliable current measurements.

VI. ECRA Performance for Different Propellants

Various gases (xenon, iodine, argon, and nitrogen) have been tested for several thruster operating conditions, producing a large database useful for performance estimation. The thruster has been operated at different input powers, from 20 W to 45 W, and at various flowrates (between 0.10 and 0.45 mg/s). In the case of iodine, two levels of pressure have been tested: around 10^{-5} mbar (without cryogenic system), noted as I_2 in the plots, and around 10^{-6} mbar (with cryogenic system), noted as $I_{2,cryo}$ in the plots.

A. Thruster floating potential

As mentioned in section V-B, the thruster is electrically floating. This ensures that the plume remains current-free, so that no net current is drawn from the thruster. Under this condition, the thruster floats at the floating potential (V_T), which can provide information about thruster performance as it is related to ion kinetic energy estimation. The thruster floating potential is a global, integrated value, as the conductive walls of the thruster average out local plasma effects within the source. It can be express as:

$$V_T = \langle V_{\text{plasma}} \rangle - \Delta V_{\text{sheath}}, \tag{9}$$

where $\langle V_{\text{plasma}} \rangle$ is the average plasma potential in the source region and ΔV_{sheath} is the voltage drop across the plasma sheath at the thruster wall.

Along the axial direction, there is an electrostatic potential drop from the average plasma potential, $\langle V_{\text{plasma}} \rangle$, in the thruster source to the far-field potential, $V^{\infty} = 0$. In ground-based testing, this boundary condition is found at the facility wall facing the thruster exhaust plane. The total electrostatic potential drop is $\Delta V_{\text{nozzle}} = \langle V_{\text{plasma}} \rangle - V^{\infty} = \langle V_{\text{plasma}} \rangle$. The electric field resulting from this potential drop is responsible for the ion acceleration, thereby enabling thrust generation. Assuming that this potential drop is entirely converted into ion kinetic energy (i.e., $E_{\text{i}} \simeq \langle V_{\text{plasma}} \rangle$), the ion velocity can be expressed as:

$$v_i = \sqrt{\frac{2e\langle V_{\text{plasma}} \rangle}{M}} \tag{10}$$

The remaining quantity in Eq. 9, ΔV_{sheath}, is not straightforward to estimate, as it strongly depends on various factors such as plasma parameters inside the source (electron density and temperature), magnetic field geometry and strength, and wall surface properties. As a result, the relationship between V_T and E_i is not known *a priori*. In the case of ECRA thrusters, it has been shown that the ratio V_T/E_i remains approximately constant for a given thruster and vacuum chamber configuration while being sensitive to the background pressure [8] and change of facility. In this work, we did not have access to ion energy measurements, nor to a pre-existing database of V_T/E_i values. To proceed in our analysis and provide a first order estimation of the ion energy, we assume a ratio of $V_T/E_i = 0.8$ based on available experimental data [8] for the remainder of this paper. While this approach enables us to estimate performance trends for a given gas and pressure level, it yields an uncertainty on the absolute thrust values obtained here and does not allow for accurate comparisons between different propellant gases. For such comparisons, direct ion energy measurements are necessary.

Figure 4 shows the thruster floating potential at an operating power of 30 W for the tested propellants. In agreement with previous observations [8], the floating potential decreases when increasing the flowrate for all gases. Under conditions where only the turbomolecular pump is active, the floating potential is higher for argon and nitrogen than for xenon and iodine. When the cryopump is turned on, the floating potential increases during iodine operation. This behavior reflects the fact that the thruster potential tends to increase as the background vacuum pressure is reduced [8].

B. Thrust

The thrust produced is evaluated indirectly by integrating the momentum carried by the ion flux on a hemisphere around the thruster [14], under the assumption that thrust is mainly due to ions contribution. This assumption is justified by the fact that (i) electron mass is negligible compared to ion mass (which is 10^5 larger than electron mass in the case of xenon and iodine ions), and that (ii) neutral particles are ejected at approximately their thermal velocity, which is 1 to 2 orders of magnitude smaller than the ion ejection velocities around

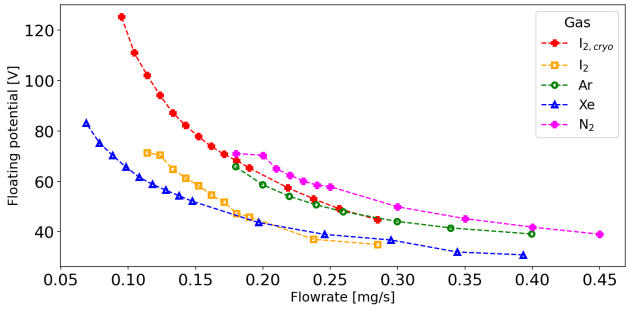

Fig. 4. Thruster floating potential as functions of mass flowrate for different gases at 30 W.

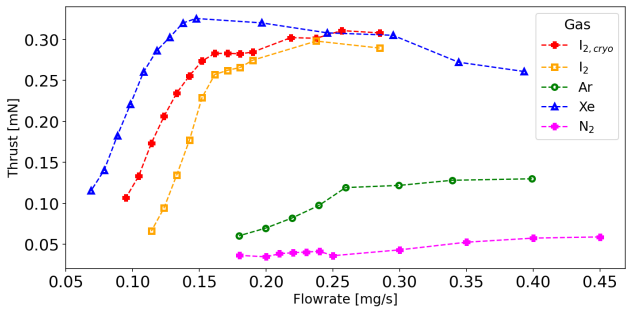

Fig. 5. Thrust as a function of mass flowrate for different gases at 30 W of power.

10 km/s [15]. The local thrust δT_z on a surface element δS of the hemisphere centered at the thruster is written as:

$$\delta T_z = m_i n_i v_i^2 \cos(\theta)\, \delta S, \tag{11}$$

where m_i, n_i, v_i are the ion mass, density, and velocity. In axisymmetric geometry, the total thrust becomes:

$$T = \pi \rho^2 \frac{m_i v_i}{e} \int_{-\frac{\pi}{2}}^{\frac{\pi}{2}} j_i \cos(\theta) |\sin(\theta)|\, d\theta, \tag{12}$$

where ρ is the distance of the probe to the center of rotation and $j_i = e n_i v_i$ is the ion current density. The ion velocity v_i is derived from the thruster floating potential as detailed in the previous section and introduces an uncertainty in the indirect thrust estimation.

Figure 5 shows the evolution of thrust against mass flowrate at a fixed input power of 30 W. Among the tested propellants, nitrogen produces the lowest thrust, around 50 µN. Argon exhibits higher thrust values, ranging from 75 to 200 µN, increasing steadily with flowrate. Xenon and iodine deliver the highest thrust, varying between 150 and 350 µN, and display similar trends in the evolution of thrust as a function of flowrate. In the case of xenon and iodine, thrust increases rapidly between 0.08 and 0.15 mg/s, then tends to saturate or even slightly decrease at higher flowrates, particularly for xenon. The measured thrust for iodine does not appear to be significantly influenced by the pumping speed; however, this is likely due to the assumptions made in estimating the ion energy, E_i.

TABLE II
MEASURED PERFORMANCE FOR IODINE AND XENON AT DIFFERENT INPUT POWERS.

Gas	ϕ [mg/s]	Power [W]	Pressure [mbar]	T [mN]	TTPR [mN/kW]	I_b [mA]	I_{sp} [s]	η_m [%]	η_d [%]	η_e [%]	η_T [%]	V_T [V]
$I_{2,cryo}$	0.24	25	1.54e-06	0.21	8.4	19.5	91.5	11.0	84.6	4.83	0.4	49
$I_{2,cryo}$	0.16	25	1.10e-06	0.19	7.6	15.1	120.6	12.4	85.1	5.0	0.5	66
$I_{2,cryo}$	0.24	45	1.54e-06	0.43	9.5	39.3	185.1	22.0	83.3	5.6	0.9	52
$I_{2,cryo}$	0.16	45	1.32e-06	0.39	8.6	28.3	246.4	23.4	83.7	6.3	1.0	81
I_2	0.24	25	1.21e-05	0.22	8.9	24.3	97.0	13.6	83.3	4.5	0.4	37
I_2	0.16	25	5.28e-06	0.20	7.9	19.2	125.8	15.8	83.4	4.4	0.5	46
I_2	0.24	45	1.25e-05	0.38	8.5	44.0	166.4	24.7	80.5	4.3	0.7	36
I_2	0.16	45	5.72e-06	0.38	8.5	36.1	244.8	29.8	80.7	5.2	1.0	53
Xe	0.2	25	3.52e-05	0.26	10.2	26.9	132.6	18.6	78.8	5.7	0.7	43
Xe	0.13	25	2.28e-05	0.22	8.7	21.0	174.2	22.4	78.1	5.5	0.7	52
Xe	0.2	45	3.52e-05	0.42	9.4	43.1	218.7	29.8	78.3	5.5	1.0	46
Xe	0.13	45	2.44e-05	0.41	9.0	37.2	324.0	39.6	77.7	6.0	1.4	58

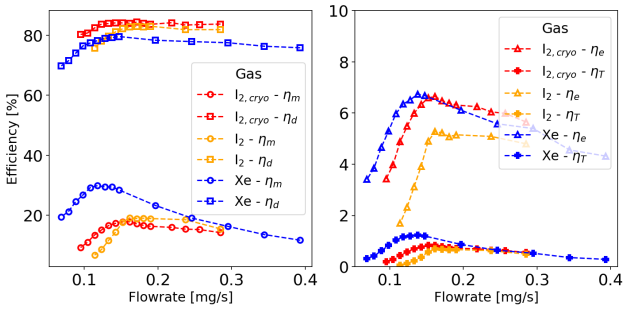

Fig. 6. Efficiencies η_m, η_e, η_d, and η_T against mass flowrate for xenon and iodine at 30 W.

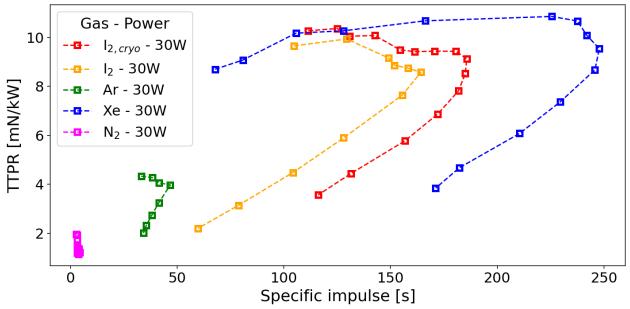

Fig. 7. TTPR vs. specific impulse (I_{sp}) at 30 W input power. The mass flowrate varies as in the abscissa of Fig. 5.

C. Thruster efficiencies

Figure 6 compares mass (η_m), divergence (η_d), energy (η_e), and total thrust (η_T) efficiencies obtained for iodine and xenon at 30 W across the tested range of flowrates. Globally, all efficiencies exhibit a bell-shaped trend, peaking around 0.13-0.15 mg/s for both propellants, with comparable values between xenon and iodine. Mass efficiency (Fig. 6, left) peaks at approximately 30% for xenon and 20% for iodine (at higher and lower pressure, i.e., with and without cryogenic pumping). This slightly lower value for iodine may be attributed to its molecular nature and additional chemical losses absent in monatomic xenon. Consistently with previous studies [16], divergence efficiency shows minimal sensitivity to flowrate or propellant type, remaining between 70 and 85% over the entire flowrate range. Energy efficiency (Fig. 6, right) reaches a maximum of around 5-6% for both gases. Iodine at lower pressure performs better than iodine at higher pressure, most likely due to higher ion energy obtained when decreasing the background pressure. Total efficiency (Fig. 6, right), which reflects the combined contribution of the above metrics, peaks at around 1% near 0.13-0.15 mg/s for both iodine and xenon, suggesting this range as a likely optimal operating point. At higher flowrates, thrust efficiency drops mainly due to reduced mass utilization. At lower flowrates, performance is likely limited by under-utilization of input power: η_e decreases by approximately $\simeq$ 50% for iodine and $\simeq$ 30% for xenon when the flowrate decreases from 0.15 mg/s to 0.08 mg/s. These data can be found in Table II.

Figure 7 presents the evolution of TTPR against the specific impulse (I_{sp}) for all tested propellant at 30 W of input power. Xenon delivers the highest overall performance, with I_{sp} up to 240 s and TTPR above 10 mN/kW with a broad operating range. Iodine with cryogenic pumping (i.e., at lower operating pressure) follows closely, with similar peak TTPR values at a lower I_{sp} of around 180 s. Iodine at higher pressure exhibits reduced performance, with a peak $I_{\text{sp}} \simeq 150$ s, reflecting the degradation of ECRA performance when operating pressure increases. Argon performs significantly worse in both metrics, with lower I_{sp} and TTPR values. Nitrogen exhibits the lowest overall performance, with TTPR below 2 mN/kW and very low I_{sp}. These results highlights iodine as a viable alternative to xenon, offering competitive TTPR and specific impulse.

Finally, Table II provides a comparative overview of xenon and iodine performance for different input powers and flowrates. For iodine, both low- and high-pressure conditions are reported, corresponding to operation with and without cryogenic pumping, respectively.

VII. IMPACT OF IODINE PLASMA COMPOSITION ON ECRA THRUSTER PERFORMANCE ASSESSMENT

Iodine plasmas typically contain various ion species, including both atomic and molecular ions, which can be singly or multiply charged [3]. In this study, we perform a preliminary analysis of the impact of the iodine plasma composition on the indirect thrust evaluation. We limit the analysis to the presence of two ion species: the atomic singly-charged ion I^+ (referred to as species I in the following) and the molecular singly-charged ion I_2^+ (referred to as species II in the following).

In the following, we consider that both species have the same kinetic energy at the point of measurement in the far-field

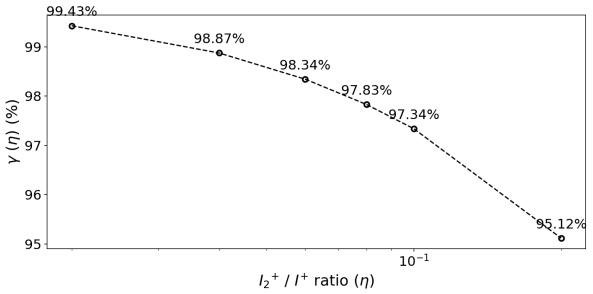

Fig. 8. Ratio of measured to total thrust, γ against the density ratio η.

of the thruster source ($E_{I,i} = E_{II,i}$) since they are accelerated by the same electrostatic potential drop along the magnetic nozzle. Also, taking into account that the mass of I_2^+ is twice the mass of I^+, their velocities are related by the following relationship:

$$v_{\mathrm{II}} = \frac{v_{\mathrm{I}}}{\sqrt{2}}. \tag{13}$$

We define the density ratio between the two species as:

$$\eta = \frac{n_{\mathrm{II}}}{n_{\mathrm{I}}}. \tag{14}$$

The measured thrust T^{meas} indirectly estimated from the integration of the measured ion current density (see section VI.B) accounts for the contributions of both I^+ and I_2^+. Since these ions differ in mass and velocity, their individual effects on the measured current density must be considered. Rewriting Eq. 12 and considering the effect of singly and doubly charged ions, the indirect thrust can be expressed in the following general form:

$$T^{\mathrm{meas}} = T_{\mathrm{I}} \left(1 + \frac{\eta}{\sqrt{2}}\right), \tag{15}$$

where T_{I} is the contribution of only I^+ to the indirect thrust. The total thrust T^{tot}, which would be obtained through a direct measurement method such as a thrust stand, includes the full contribution of both I and II species and can be written as:

$$T^{\mathrm{tot}} = T_{\mathrm{I}}(1 + \eta). \tag{16}$$

By evaluating the ratio between the measured and total thrust, it is possible to quantify the relative error introduced when estimating the thrust using the indirect method and assuming a certain ratio between I and II species:

$$\gamma(\eta) = \frac{T^{\mathrm{meas}}}{T^{\mathrm{tot}}} = \frac{1 + \frac{\eta}{\sqrt{2}}}{1 + \eta}. \tag{17}$$

The trend of γ as a function of the density ratio η is illustrated in Figure 8. The density ratio η is varied between 0.02 and 0.2, assuming that species I is predominant, in agreement with measurements made by Szabo *et al.* [2] in the plume of a Hall Effect Thruster. Figure 8 shows that the thrust estimated from ion current measurements may underestimate the actual thrust (Eq. 17) by up to 5% when $\eta = 0.2$. The effect of varying the relative concentration of molecular over atomic singly-charged ions on the indirect thrust estimation using ion flux probe is therefore limited. The composition of the ECRA thruster plume will be the focus of further studies to confirm this conclusion.

VIII. Conclusion and future works

An experimental setup has been developed to support iodine operations in ECRA thrusters. Experimental tests with various propellants confirm that iodine is a viable alternative to xenon for electric propulsion systems. Iodine performance figures are comparable to those of xenon which is highly promising. This work has identified key challenges in accurately assessing performance of iodine-fueled thrusters. In particular, precise measurements of ion energy and plasma composition are essential to improve the accuracy of indirect thrust estimation. Future investigations will focus on the fundamental physics of iodine plasmas, with special emphasis on their electronegative nature, species composition, and specific discharge characteristics. The development of diagnostics for plasma composition and a dedicated thrust stand will enhance the accuracy and reliability of thrust and thruster performance measurements. Additionally, testing in larger vacuum facilities with higher pumping capacities will be necessary to evaluate the representative performance of ECRA thruster operating with iodine under more realistic space-like conditions.

Acknowledgments

This work was supported by ANR under the project *EPPSI*, grant number ANR-CE51-23-0020 and by ONERA and CNES under the common project *Iodine Electric Propulsion*, grant number 5800003318.

References

[1] A. C. Hillier, Air Force Institute of Technology, Tech. Rep., 2011.
[2] J. Szabo, B. Pote, S. Paintal, *et al.*, *Journal of Propulsion and Power*, vol. 28, no. 4, 2012.
[3] J. Szabo, M. Robin, S. Paintal, B. Pote, V. Hruby, and C. Freeman, IEPC–2013–311, 2013.
[4] P. Grondein, T. Lafleur, P. Chabert, and A. Aanesland, *Physics of Plasmas*, vol. 23, no. 3, 2016.
[5] K. Holste, W. Gärtner, D. Zschätzsch, *et al.*, *The European Physical Journal D*, vol. 72, no. 9, 2018.
[6] J. Yang, S. Jia, Z. Zhang, *et al.*, *Plasma Science and Technology*, vol. 22, no. 9, 2020.
[7] D. Rafalskyi, J. M. Martínez, L. Habl, *et al.*, *Nature*, vol. 599, no. 7885, 2021.
[8] T. Vialis, Ph.D. dissertation, Sorbonne Université, 2018.
[9] F. Cannat, T. Lafleur, J. Jarrige, P. Chabert, P. Q. Elias, and D. Packan, *Phys. Plasmas*, vol. 22, 2015.
[10] J. Jarrige, P.-Q. Elias, and D. Packan, *IEPC–2013–420*, 2013.
[11] S. Peterschmitt and D. Packan, *Journal of Propulsion and Power*, vol. 37, no. 6, 2021.
[12] V. Désangles, D. Packan, J. Jarrige, *et al.*, *Journal of Electric Propulsion*, vol. 2, no. 1, 2023.
[13] F. Boni, V. Désangles, P.-Q. Elias, J. Jarrige, and D. Packan, *IEPC–2024–792*, 2024.
[14] R. Pioch, V. Désangles, and P. Chabert, *Physics of Plasmas*, vol. 31, no. 4, 2024.
[15] S. Correyero, J. Jarrige, D. Packan, and E. Ahedo, *Plasma Sources Science and Technology*, vol. 28, no. 9, 2019.
[16] A. J. Sheppard and J. M. Little, *Journal of Propulsion and Power*, vol. 39, no. 2, 2022.